MRTD ANALYSIS OF DIELECTRIC CAVITY STRUCTURES

Rob Robertson, Emmanouil Tentzeris, Michael Krumpholz, Linda P.B. Katehi

Radiation Laboratory, Department of Electrical Engineering and Computer Science
University of Michigan, Ann Arbor, MI 48109-2122

ABSTRACT

Multiresolution time domain (MRTD) analysis is applied to model anisotropic dielectric material. In particular, an MRTD scheme based on scaling functions only is used to analyze different types of resonant cavity structures. The results agree very well with those obtained by FDTD, FEM and integral equation methods. MRTD allows for considerable savings in memory and computational time in comparison to FDTD, while maintaining the same accuracy of the results.

INTRODUCTION

The method of moments is a mathematically correct approach for the discretization of integral and partial differential equations. It has been shown in [1] that the method can be used to derive Yee's FDTD scheme using pulse functions for the expansion of the unknown fields. Since the method of moments allows for the use of a complete set of orthonormal basis functions, it is possible to derive time domain schemes based on the expansion of the fields in scaling and wavelet functions and based on multiresolution analysis, respectively [2, 3]. These multiresolution time domain(MRTD) schemes have highly linear dispersion characteristics, allowing MRTD to provide excellent accuracy in electromagnetic computation for discretizations close to the Nyquist limit. MRTD exhibits significant improvements over FDTD and good convergence with FEM and IE methods in calculating resonant frequencies and field patterns.

MODELLING ANISOTROPIC DIELECTRIC MATERIAL

To model anisotropic dielectric material we separate Maxwell's first vector equation in:

$$\nabla \times \mathbf{H} = \frac{\partial \mathbf{D}}{\partial t} \tag{1}$$

and

$$\mathbf{D} = \boldsymbol{\epsilon}(\vec{r}, t)\, \mathbf{E} \quad , \tag{2}$$

where $\mathbf{D}$ represents the electric flux vector and $\boldsymbol{\epsilon}(\vec{r}, t)$ the space- and time-dependent permittivity tensor. These equations can be discretized using scaling and pulse functions in space and time domain as expansion factors in the method of moments [3]. The use of non-localized basis functions cannot accomodate localized boundary conditions and cannot allow for a localized modelling of the material properties. To overcome this difficulty, the image principle is used to model perfect electric boundary conditions, as described below. As for the description of material parameters, the constitutive relations are discretized accordingly so that the relationships between the electric/magnetic flux and the electric/magnetic field are given by matrix equations.

In the principal coordinate system, the permittivity tensor $\boldsymbol{\epsilon}$ for symmetric media is given by

$$\boldsymbol{\epsilon}(\vec{r}, t) = \begin{bmatrix} \varepsilon_x(\vec{r}, t) & 0 & 0 \\ 0 & \varepsilon_y(\vec{r}, t) & 0 \\ 0 & 0 & \varepsilon_z(\vec{r}, t) \end{bmatrix} \quad . \tag{3}$$

In this case, eq. (2) may be written in the form of three scalar cartesian equations as

$$D_x = \varepsilon_x(\vec{r}, t)\, E_x \tag{4}$$

TH 3F

0-7803-3246-6/96/$5.00 © IEEE

$$D_y = \varepsilon_y(\vec{r},t)\, E_y \quad (5)$$

$$D_z = \varepsilon_z(\vec{r},t)\, E_z \quad (6)$$

The discretization of eqs. (4), (5) and (6) for field expansions using only scaling functions in space domain is discussed in [3]. Assuming

$$\varepsilon(\vec{r},t) = \varepsilon(x)\,\varepsilon(y)\,\varepsilon(z)\,\varepsilon(t) \quad (7)$$

yields

$${}_kD^{\phi x}_{l+1/2,m,n} = \sum_{k',l',m',n'=-\infty}^{+\infty} \varepsilon^{\phi x}_{(x)l+1/2,l+1/2'}\, \varepsilon^{\phi x}_{(y)m,m'}\, \varepsilon^{\phi x}_{(z)n,n'}\, \varepsilon^{x}_{(t)k,k'}\; {}_{k'}E^{\phi x}_{l'+1/2,m',n'} \quad , \quad (8)$$

where the epsilon coefficients $\varepsilon^{\phi x}_{(\kappa)m,m'}$ and $\varepsilon^{x}_{(t)k,k'}$ are integrals given by

$$\varepsilon^{\phi x}_{(\kappa)m,m'} = \frac{1}{\Delta\kappa}\int \phi_m(\kappa)\,\varepsilon_x(\kappa)\,\phi_{m'}(\kappa)\,d\kappa \quad (9)$$

and

$$\varepsilon^{x}_{(t)k,k'} = \frac{1}{\Delta t}\int h_k(t)\,\varepsilon_x(t)\,h_{k'}(t)\,dt \quad , \quad (10)$$

with $\kappa = (x,y,z)$. The functions $\phi_m(\kappa)$ are Battle-Lemarie scaling functions and $h_k(t)$ are pulse functions. The indices l, m, n and k are the discrete space and time indices related to the space and time coordinates via $x = l\Delta x$, $y = m\Delta y$, $z = n\Delta z$ and $t = k\Delta t$, where Δx, Δy, Δz and Δt represent the space and time discretization intervals in x–, y–, z– and t–direction.

ANALYSIS OF RESONANT CAVITY STRUCTURE

For the evaluation of the integrals (9), we use a simple representation of the scaling function in terms of cubic spline functions [3]. The first structure in our analysis is a resonant cavity that is filled one-quarter with a dielectric material(see Fig. 1). The cavity has the dimensions $1m \times 2m \times 1.5m$, and the dielectric material has a relative dielectric constant equal to 64. Note that for this structure it is only necessary to calculate the epsilon coeffcients for the y–direction, since the structure is homogeneous with respect to the x– and z– directions. The electric field components tangential to the dielectric interface, ${}_{k'}E^{\phi x}_{l',m',n'}$ and ${}_{k'}E^{\phi z}_{l',m',n'}$ are related to ${}_kD^{\phi x}_{l,m,n}$ and ${}_kD^{\phi x}_{l,m,n}$ by the tangential epsilon(ε) coefficients $\varepsilon^{\phi x}_{(y)}$ and $\varepsilon^{\phi z}_{(y)}$ respectively. Additionally, the electric field component normal to the dielectric interface ${}_{k'}E^{\phi y}_{l',m',n'}$ is related to ${}_{k'}D^{\phi y}_{l',m',n'}$ by the normal (ε) coefficient $\varepsilon^{\phi y}_{(y)}$. To model the structure in Figure 1 the image principle is applied, thus replacing the structure in Figure 1 by the structures shown in Figures 2 and 3 respectively. The tangential ε coefficients now relate ten ${}_{k'}E^{\phi x}_{l',m',n'}$ components to ten ${}_kD^{\phi x}_{l,m,n}$ components through a 10×10 matrix. The image principle applies odd symmetry of the tangential electric fields. Thus the five tangential electric field components in the image resonator are linearly dependent on the five tangential electric field components in the original resonator. This allows the elimination of the field components in the image resonator, reducing the 10×10 matrix to a 5×5 matrix, which is used in eq. (8). Similarly, the 12×12 matrix of the normal ε coefficient is reduced to a 6×6 matrix using even symmetry for the normal electric field component. Note that a general description of ε coefficients in eq. (9) allows for an arbitrary positioning of the dielectric interface.

The MRTD method for the structure in Figure 1 at a discretization of $2 \times 6 \times 3$ proved to be the closest approximation to analytic values. This is due to the fact that a discretization of $2 \times 4 \times 3$ is exactly at the Nyquist criterion for the variation of ε in the y–direction (one sampling point in the dielectric material). MRTD results are compared to analytic values and the results obtained by Yee's FDTD scheme in Table 1. The time discretization interval $\Delta t = 0.9 \cdot 10^{-10} s$ was identical for both schemes. This time discretization interval was chosen to maximize the linear properties of the MRTD dispersion relation [3]. Both cases were run at 35,000 time steps. For the analysis using Yee's FDTD scheme, a mesh with $\Delta x = \Delta y = \Delta z = 0.1m$ was used resulting in a total number of 3000 grid points. In the $2 \times 6 \times 3$ analysis, a total number of 36 grid points was used, resulting in a factor of 83 memory improvement for MRTD. Additionally an improvement of a factor of 10 in computation time was found for the MRTD method.

The second structure is a metallic cavity of dimensions $2m \times 2m \times 2m$ with a small dielectric cube($\varepsilon_r = 6$) of dimensions $0.5m \times 0.5m \times 0.5m$ in one corner of the structure. Note that it is necessary to use tangential and normal ε coefficients for the x–,y–,z– directions. Due to symmetry, the ε coefficients along each direction are identical. This structure was simulated using an MRTD discretization of $8 \times 8 \times 8$ and an FDTD discretization of $60 \times 60 \times 60$, resulting in a memory savings of 420. The time discretization interval is $\Delta t = 9.0 \cdot 10^{-11} s$ for MRTD and $\Delta t = 2.0 \cdot 10^{-11} s$ for FDTD. Both cases were run for 50,000 time steps. The first resonant frequency was found to be 105.1 MHz for FDTD and 106.1 MHz for MRTD. Since FDTD has negative and MRTD positive dispersion error [2, 3], the analytic value is between 105.1 and 106.1 MHz. Due to the evaluation of the full three–dimensional matrix equation (9) running time was the same for both methods.

The third structure is a $4cm \times 3cm \times 2cm$ resonant cavity with a dielectric perturbation in the center of one of the faces. We define r to be the ratio between the side of the dielectric cube and the side of the resonant cavity along x, y, or z (see Fig.4). An MRTD discretization of $8 \times 8 \times 8$ is compared with tetrahedral FEM [4] and an integral equation method [5] for r=0.15, 0.20 and 0.25. For each value of r, the time discretization interval in MRTD is $\Delta t = 3.0 \cdot 10^{-12} s$ and the number of time steps used was 60,000. Note that the results calculated by the MRTD scheme are compared to results derived by two conventional frequency domain techniques. The IE/MoM method has a discretization of $3 \times 3 \times 3$ only in the dielectric, while in FEM the whole cavity is discretized with 1500 tetrahedrons. As can be seen in Table 2, values derived by these techniques agree very well.

Figures 5 and 6 show plots of $E^{\phi y}$ calculated using MRTD with a discretization of $8 \times 8 \times 8$ for r=0.20. Field values can be evaluated for any number of intermediate points. Figure 5 shows the amplitudes of the scaling functions calculated by MRTD. Figure 6 shows field distributions using three intermediate points resulting in a higher field resolution of $24 \times 24 \times 24$. The use of pulse functions in FDTD results in only one field value per discretization cell, while in MRTD scaling functions imply field variations within the discretization cell. This yields a higher field resolution for a higher number of intermediate points.

CONCLUSION

MRTD schemes based on orthonormal wavelet expansions have been derived and applied in the numerical analysis of simple resonant cavity structures. It has been shown the MRTD scheme using Battle–Lemarie scaling functions provides results with excellent correspondance with the FDTD, FEM and IE methods. Compared to Yee's FDTD scheme, our examples suggest computer savings of two orders with respect to memory requirements.

ACKNOWLEDGEMENTS

This work has been made possible by a scholarship of the NATO science committee through the German Academic Exchange Service and by the U.S. Army Research Office. The authors also wish to thank K. Sabetfakhri and J. Yook.

References

[1] M. Krumpholz, P. Russer, "Two–Dimensional FDTD and TLM", Int. Journal of Num. Modelling, vol. 7, no. 2, pp. 141-153, February 1993.

[2] M. Krumpholz, L.P.B. Katehi, "New Prospects for Time-Domain Analysis", IEEE Guided Wave Letters, pp. 382-384, November, 1995.

[3] M. Krumpholz, L.P.B. Katehi, "MRTD: New Time Domain Schemes Based on Multiresolution Analysis", Submitted to the IEEE Transactions on Microwave Theory and Techniques, May 1995.

[4] J. Yook et. al., "A Study of Hermetic Translations for Microwave Transitions", IEEE MTT-S International Microwave Symposium, pp. 1579-1582, May 1995.

[5] K. Sabetfakhri, "Cavity-based Dielectric Constant Measurement: A Full Wave Approach", Submitted to the 1996 IEEE Microwave Symposium.

Analytic (MHz)	27.290	37.136	42.343
FDTD ($10 \times 20 \times 15$)	27.250	37.000	42.200
FDTD Relative Error	–0.146%	–0.366%	–0.337%
MRTD ($2 \times 6 \times 3$)	27.370	37.370	42.420
MRTD Relative Error	0.292%	0.599%	0.299%

Table 1: Resonant Frequency data for a cavity one–quarter filled with dielectric material

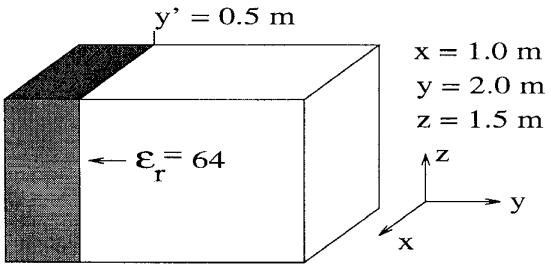

Figure 1: **Quarter-Filled Dielectric Resonator**

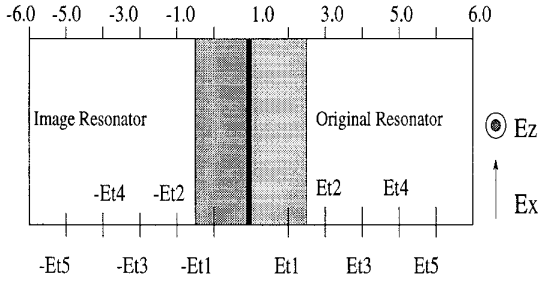

Figure 2: **Tangential ϵ Components**

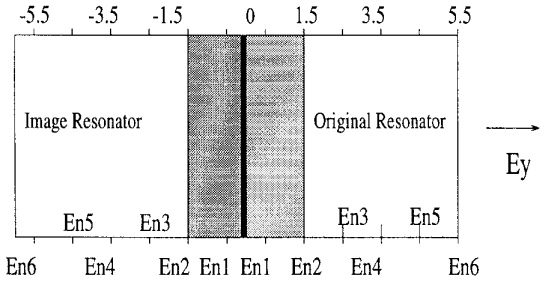

Figure 3: **Normal ϵ Components**

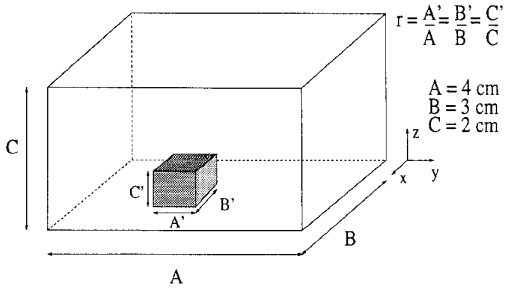

Figure 4: **Cavity Resonator with a varying dielectric perturbation**

r	IE/MoM(GHz)	FEM	MRTD
0.15	6.1535	6.1125	6.20
0.20	6.02	5.9125	5.95
0.25	5.840	5.740	5.85

Table 2: **Resonant Frequencies for a resonator with a varying dielectric perturbation**

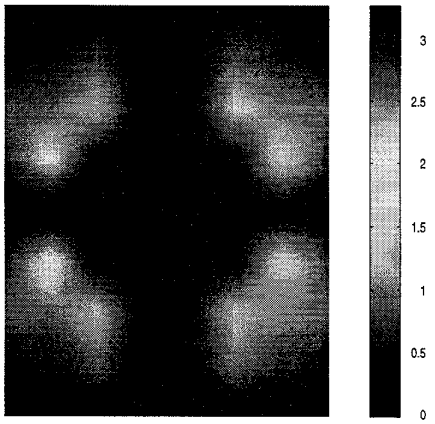

Figure 5: **Ey Field Pattern for r=0.20, MRTD 8x8x8, w/o Scaling Function Interpolation**

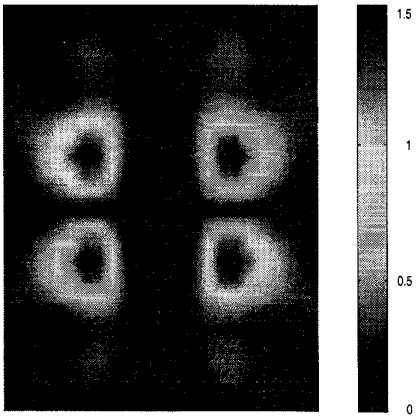

Figure 6: **Ey Field Pattern for r=0.20, MRTD 8x8x8, w/Scaling Function Interpolation**